**References**

1. A. Bellare, A. Bistolfi, K. Simis & L. Pruitt, Proceedings of *UHMWPE for arthroplasty.* Torino, Italy, 19.5.2003, pp.33-51 and references therein.
2. F. Shen, H. & McKellop, Proceedings of *UHMWPE for arthroplasty.* Torino, Italy, 19.5.2003, pp.73-86 and references therein.
3. G. Lewis, *Biomaterials* **22** (2001), 371-401.
4. M. Nevoralova, J. Mikesova, J. Baldrian & Z. Horak, *Polym. Advan. Technol.* **14** (2003) 802-806.
5. Kurtz S M, Muratoglu O K, Evans M & Edidin A A, *Biomaterials* **20** (1999) 1659-1688.
6. M. Šlouf, H. Synková, J. Baldrian, J. Kovářová, A. Marek, H. Dorschner & M. Stephan: Structural changes in irradiated UHMWPE. In preparation.
7. V. Premnath, A. Bellare, E. W. Merrill, M. Jasty & W. H. Harris, *Polymer* **40** (1999) 2215–2229.
8. N. D. Jordan, D. C. Bassett, R. H. Olley & N. G. Smith, *J. Biomed. Mater. Res.* **55** (2001) 158-163.
9. http://www.volny.cz/mirek.slouf/PROG/MDFT/mdft.htm.
10. http://www.perl.com.
11. http://www.boutell.com/gd.
12. http://stein.cshl.org/WWW/software/GD.
13. http://www.gnuplot.info.
14. H. Synkova, M. Slouf, J. Baldrian, A. Sikora, J. Kovarova, M. Stephan: Proceedings of: *World Polymer Congress Macro 2004*, Paris, France, 4.7 - 9.7.2004. p. 114.
15. R. Ryong-Joon: Methods of X-ray and Neutron Scattering. London, 2000. Oxford Univeristy Press. Chapter 1.
16. A. R. Clarke & C. N. Eberhardt: Microscopy Techniques for Materials Science. Cambridge, England, 2000. Woodhead Publishing Ltd. p. 145.
17. http://homepages.inf.ed.ac.uk/rbf/HIPR2/fourier.htm.
18. http://www.imagemagick.org/.
19. http://www.imagemagick.org/script/perl-magick.php

# STRUCTURE CHARACTERISTICS OF Al-PLATES JOINED BY FRICTION STIR WELDING

**N. Ganev[1], J. Marek[1], P. Sláma[2]**

*[1]Department of Solid State Engineering, Faculty of Nuclear Sciences and Physical Engineering, Czech Technical University in Prague, Trojanova 13, 120 00 Prague 2, Czech Republic*
*[2]Research Institute for Metals Ltd., Panenské Břežany, 250 70 Odolena Voda, Czech Republic*

**Keywords**
Key words: X-ray diffraction, residual stresses, orientation distribution function (ODF), Friction Stir Welding (FSW), back reflection patterns, inhomogeneous fields, metallographic analysis

**Abstract**
The aim of the contribution is to give information about Friction Stir Welding (FSW), an emerging technology of joining metals that offers benefits over traditional fusion welding processes. The both residual stress and texture distribution of an AlSi1MgMn alloy FSW joint have been determined by means of X-ray diffraction. The structure of the weld was observed under an optical microscope. The results of both the back reflection "mapping" of the sample surface and metallographic analysis show that while the structure of the basic material is very coarse-grained, the material of the weld is noticeably fine-grained and the boundary between the both structures is well pronounced. An inhomogeneous field of state residual stress was found on the weld surface with predominant tensile stresses. The asymmetric courses of residual stress distributions are, most probably, a result of the asymmetry of the FSW process. The observed qualitative difference between the texture on the weld surface and the texture in the middle of its thickness could be explained by different cooling rates of these volumes.

The presented results of X-ray diffraction and metallographic analysis confirm that although FSW has been put to use in production of boats and space launch components, there is still a good deal to be studied about the basic mechanism and the details of the process.

## 1. Friction stir welding

### 1.1 Introduction

Friction stir welding (FSW) is a newly developed method of solid phase welding invented in the early 1990s by The Welding Institute (TWI) in Cambridge, United Kingdom [1]. It uses a relatively simple process in which a specially shaped cylindrical tool is rotated and plunged into the joint line between the pieces to be welded. The frictional heat generated by the welding tool and the surrounding material causes softening and allows the tool to be moved along the joint line. The material is plasticized and transferred from the leading edge of the tool to the trailing edge, leaving a solid-phase bond between the two pieces (Fig. 1). The process may be described as a combination of in situ extrusion and forging.

Friction-stir-welded materials have a characteristic through-thickness cross section illustrated in Fig. 1.The weld forms a consolidated nugget of fine-grained, fully recrystallised material surrounded by a thermo-mechanically affected zone (TMAZ) which usually has a significantly different microstructure. Further away from the weld is a heat-affected zone (HAZ), with the unaffected base material on the outside. The advancing zone is the side of the base material, where the motion and rotation direction of the tool are in the same direction. On the retreating zone the rotation direction is opposite to the tool movement (Fig. 1).

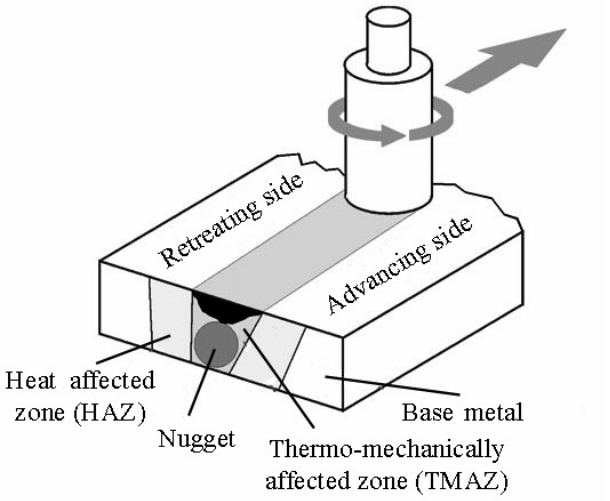


**Fig. 1**. Schematic drawing of the FSW process with the characteristic through-thickness cross section structure.

### 1.2. Process advantages and limitations

The majority of the process benefits stem from the fact that FSW is a solid-state process:

- Because there is no melting of the material, the majority of problems normally associated with conventional welding are eliminated, including porosity, solidification cracking, and shrinkage.
- Since the shrinkage associated with the liquid/solid transformation is eliminated, distortion and residual stress are minimized.
- The process requires no filler material, so parent metal chemistry is maintained with no chemical segregation.
- FSW has the ability to join materials that are difficult to fusion-weld.
- Although the technique is more reliable and maintains higher material properties than conventional welding methods, friction stir welding has had a major drawback of reliance on a single-piece pin tool. The pin is slowly plunged into the joint between two materials to be welded and rotated at high speed. At the end of the weld, the single-piece pin tool is retracted and leaves a keyhole unacceptable when welding cylindrical objects such as drums, pipes, and storage tanks.
- Another drawback is the requirement for different-length pin tools when welding materials of varying thickness.

### 1.3. Selected applications of FSW in construction area are as follows [1, 2]:

- construction equipment (truck bodies, mobile cranes),
- transportation including railroad industry (high speed trains, underground carriages),
- bridge (aluminium components),
- panels made from aluminium, copper or titanium,
- window frames,
- heat exchangers and air conditioners,
- pipe fabrication, etc.

Although FSW has been put to use in full-scale production of ferry boats and space launch components made of aluminium, there is still a great deal to be learned about the basic mechanisms and the details of the process. In addition, a great deal of work must be performed to extend the benefits of FSW to other, more refractory materials.

## 2. The sample under investigation and the experimental methods employed

Two plates of dimensions 110×175×6 mm$^3$ from the AlSi1MgMn alloy EN AW6082 were butt-welded along the longer side using Friction Stir Welding in the GKSS Research Centre in Geesthacht, Germany. The width of the resulting weld is 14 mm.

### 2.1 Mapping of the surface residual stresses of the sample

Prior to applying an X-ray diffraction method for residual stress measuring, a set of back reflection patterns was taken. The incident beam of CrK radiation collimated by a cylindrical diaphragm 1.7 mm in diameter impinged the surface perpendicularly. Diffraction rings (222) were detected on a film placed approx. 57 mm from the analysed surface.

Since the samples dimensions did not enable applying the classic "sin$^2$ " method with an – or – goniometer, the "one tilt" method with no reference substance [3] was used for residual stress determination. The incident CrK beam (1.7 mm in diameter) reached the sample surface at an angle of $_0 = 45$ in the longitudinal and transversal directions with respect to the weld centreline and surface components $_L$ and $_T$, respectively were determined. The record of the {222} Al diffraction line was obtained from a fully automated Zeiss microdensitometer and evaluated on a PC. For this experimental arrangement the surface stress can be written as

$$\frac{1}{0{,}5s_2}\,\frac{\cot\ \cos^2}{2}\,\frac{_{hkl}}{\sin 2}$$

where is the Bragg´s angle, = 90 – , D is the distance between the film and the sample, and $^{hkl} = r \quad r_2$ is the eccentricity of the diffraction ring [3]. The X ray elastic constant $0{,}5s_2 = 18.56 \ \ 10^{-6}$ [4] was used in residual stress calculations.

### 2.2 X-ray diffraction texture analysis

Two samples of dimensions 14×30×6 mm$^3$ were cut from the weld and their thickness was reduced by bottom milling to a value of 3 mm. Both the samples were arranged close to each other in the holder of a Siemens texture goniometer, so the measured area was 28×30 mm$^2$. Texture analysis on the surface of the weld as well as in the middle of its thickness was performed with CoK radiation by X-ray back reflection method on the atomic planes Al (111), (100), (110).

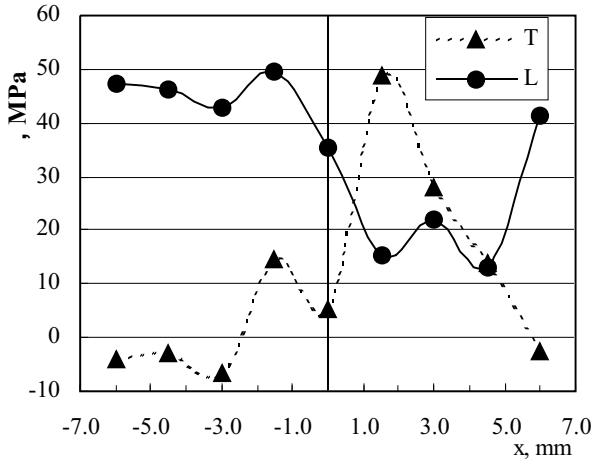


**Fig. 2.** The distribution of longitudinal (L) and transversal (T) residual stresses on the weld surface.

*ODF representation in the stereographic projection SP(001)*

The orientation distribution function (ODF) is calculated by the software *popLA* [5] as a function of Euler angles $f_2$, F, $f_1$ in the sampling of 5 degrees. These angles define a general ideal orientation of a single crystal (*hkl*)[uvw]. The pole of the planes (*hkl*) is determined by the angles $f_2$ and F, the pole of the direction [uvw] is situated on a corresponding grand circle determined by the angle $f_1$. The positions of the poles (*hkl*) and [uvw] in the standard stereographic projection are calculated from the ODF function with the aid of software ODFSP5.EXE [6], and symbols corresponding to the ODF intensity are drawn in the SP(001) plot. The poles (*hkl*) represented by lozenges are situated in quadrant IV. and poles [uvw] represented by squares are drawn in quadrants II. and III. The size of the symbol corresponds to the relative value of ODF intensity in percent. The software enables also to superimpose an ideal orientation over the experimental ODF projection.

**2.3 Metallographic analysis**

The structure of the weld was observed under the optical microscope *Nikon Epiphot 200*. The samples were first electrolytically etched in a *Barker* solution.

**3. Results and their discussion**

**3.1 Back reflection "mapping" of the sample surface**

Back reflection photographs have been taken from the weld surface as well as from the surface of the basic material. The diffraction patterns of the weld surface correspond to a fine-grained polycrystalline material with a weak preferred orientation of the crystallites, which changes only slightly from the weld centreline. On the other hand, the basic material has substantially grater crystallites that give rise to a discrete diffraction line, on whose background a low-intensive smooth pattern, corresponding to surface plastically deformed crystallites, is discernible.

**3.2 Surface distribution of macroscopic residual stresses**

The discrete character of the Al (222) diffraction line of the basic material does not enable applying the "sin$^2$ψ" method on its surface; thus the analysis of the state of residual stresses was performed only on the weld surface. The measurements carried out on 9 equidistant (the distance being 1.5 mm) positions, in both the longitudinal and transversal directions with respect to the weld centreline, are outlined in Fig. 2. Realising that the inaccuracy of the experimental values is less than 15 MPa, it is evident that:

- The surface state of residual stresses is inhomogeneous.
- The non-uniformity is more pronounced in the transversal direction ( $_T$), where the maximum span between the stress values found is approx. 60 MPa.
- Most of the stresses obtained are tensile; the few compressive stresses are less than 10 MPa.
- The courses of residual stresses $_L$ and $_T$ are different and asymmetric with respect to the weld centreline.

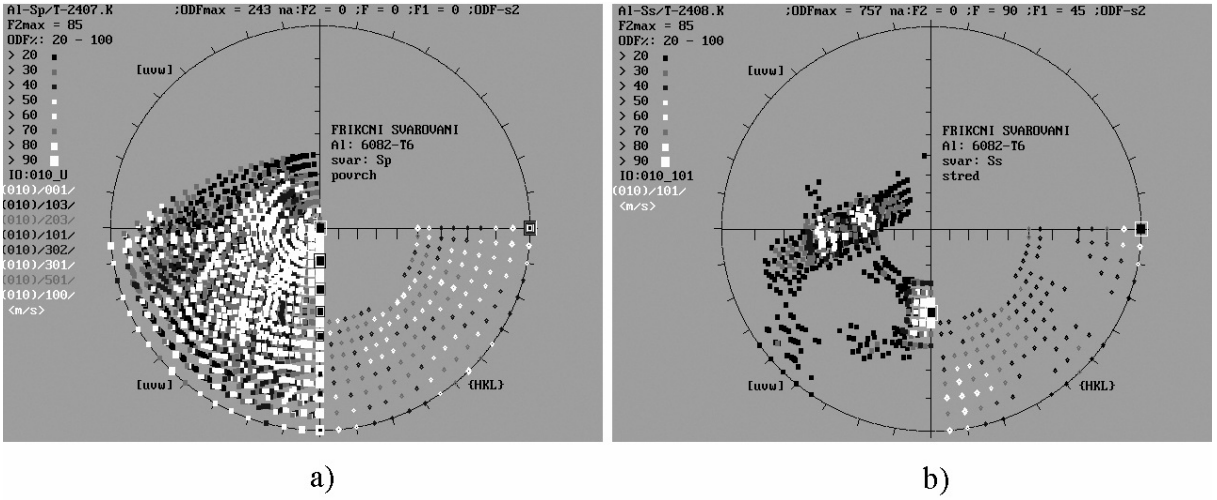


a) b)

**Fig. 3.** The orientation distribution function for the weld surface (a) and for the middle of its thickness (b) presented in the standard stereographic projection SP(001).

These findings are in good agreement with the results obtained using other techniques for residual stress determination as presented in the papers [7 – 9].

### 3.3 X-ray diffraction texture analysis

The texture distribution functions for the weld surface and for the middle of its thickness are presented in the stereographic projection SP(001) in Fig 3. As one can see

- the ***texture obtained from the weld surface*** is weak, with a maximum value of ODF obtained by *popLA* $ODF_{max}$= 243. Crystallographic directions [uvw] coplanar with the sample surface and lying in the planes (HKL) do not have any preferred orientation with respect to the weld centreline. Continual bands of poles [uvw] in quadrants II. and III. (Fig. 3a) give evidence of it.
- The ***texture in the middle of the weld thickness*** is more pronounced ($ODF_{max}$= 757) and has the ideal orientation of the (010)[101] type.

### 3.4 Metallographic analysis

Metallographic analysis of samples cut perpendicular to the weld centreline was carried out. Qualitative macro and micro-characterisation was performed. Micrographs were taken at different positions of weld cross-section. The most important observations could be summarized as follows:

- Particles of several different intermetallic secondary phases are present in the investigated alloy. The majority of the particles are phases containing the usual impurities of Al, i.e., Fe and Si and the alloying elements Mg, Mn, Zn, Si. The large amount of the $Mg_2Si$ phase has been identified in the alloy. The particles of intermetallic phases are relatively coarse, which is indicative of the fact that all the materials used were prepared from direct-chill cast alloys.
- The TMAZ and HAZ of the weld are not large and they cannot be well distinguished.
- The grains in the welds are much finer than those of the parent materials.

## 4. Conclusions

1. The results of both the back reflection "mapping" of the sample surface and metallographic analysis show that while the structure of the basic material is very coarse-grained, the material of the weld is noticeably fine-grained and the boundary between the both structures is well pronounced.

2. An inhomogeneous field of state residual stress was found on the weld surface with predominant tensile stresses (Fig. 2). The asymmetric courses of residual stress distributions are, most probably, a result of the asymmetry of the FSW process, i.e., the existence of advancing and retreating zones (see Fig. 1). The results obtained are in good correspondence with those published by other authors, e.g. in [7 – 9].

3. The qualitative difference between the texture on the weld surface and the texture in the middle of its thickness could be explained by different cooling rates of these volumes. While the rapid cooling of the surface does not "allow" the material to form a pronounced recrystallization texture, in the middle of the weld there are favourable conditions for creating a strong texture.

## References

[1] The Welding Institute Web site <http://www.twi.co.uk/>

[2] NASA Web site <http://technology.nasa.gov/>.

[3] I. Kraus, N. Ganev: Residual Stress and Stress Gradients, In: Industrial Applications of X-ray Diffraction, Eds. F.H.Chung and D.K.Smith, Marcel Dekker, Inc., New York-Basel, 2000; pp. 793-811.

[4] I. Kraus, N. Ganev: Engineering applications of diffraction analysis (in Czech), CTU Publisher, Prague 2004, 171 p.

[5] J. S. Kalend, U. F. Kocks, A. D. Rollett, H. R. Wenk: *popLA*, prefered orientation package, Los Alamos 1993.

[6] J. Marek, in: Materials Structure, Vol. 8, no. 1 (2001), pp. 29 – 37.

[7] R. V. Martins, V. Honkimäki, in: European Synchrotron Radiation Facility 2003 Highlights, ERSRF, Grenoble 2004, pp. 54 – 55.

[8] M. B. Prime, R. J. Sebring et.al., in: proceedings of the 2004 SEM X International Congress & Exposition on Experimental and Applied Mechanics, June 7 – 10, 2004, Costa Mesa, California USA, paper number 144 (CD-ROM proceedings.

[9] M. A. Sutton, A. P. Reynolds, D.-Q. Wang, C. R. Hubbard, in: Journal of Engineering Materials and Technology, Vol. 124, APRIL 2002, pp. 215 – 221.

*The research has been supported by the project MSM 6840770021.*